Politecnico di Torino

Politecnico di Torino

Master of Science in Energy and Nuclear Engineering
01FJIXY - Computational Thermomechanics
A.Y. 2025/2026

Homework 02 - Plate with Circular Hole

Tommaso COGOZZO

1 Problem statement and given data

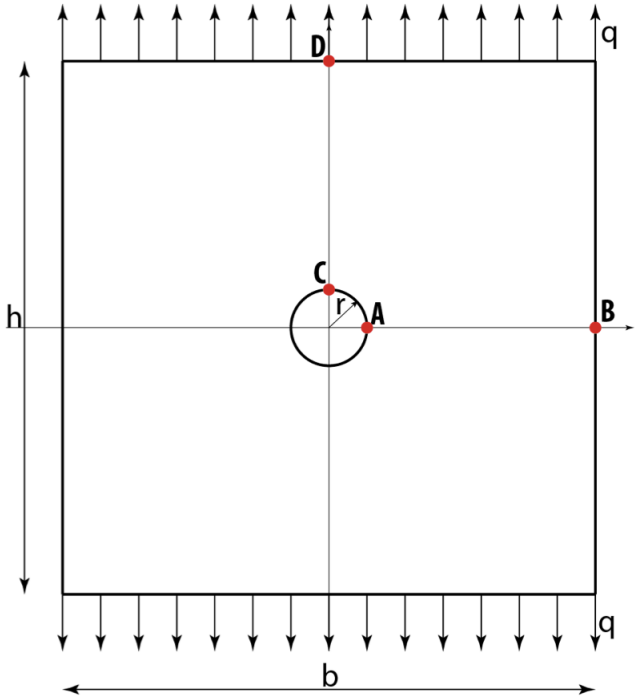

Figure 1: Plate with circular hole and a uniform load applied on the top and bottom side

Data:

- Width: $b = 0.7\,m$
- Height: $h = 0.7\,m$
- Thickness: $t = 0.01\,m$
- Hole radius: $R = 0.05\,m$
- Elasticity modulus: $E = 2.1e11\,N/m^2$
- Poisson's ratio: $\nu = 0.3$
- Applied load: $q = 2.5e6\,N/m$

2 Objective

The problem of a plate with a circular hole subjected to uniaxial tension can be solved analytically by employing the Kirsch's solutions:

$$\sigma_{rr} = \frac{P}{2}[1 - (\frac{R}{r})^2] + \frac{P}{2}[1 - 4(\frac{R}{r})^2 + 3(\frac{R}{r})^4]cos2\theta$$

$$\sigma_{\theta\theta} = \frac{P}{2}[1 + (\frac{R}{r})^2] - \frac{P}{2}[1 + 3(\frac{R}{r})^4]cos2\theta$$

$$\tau_{r\theta} = -\frac{P}{2}[1 + 2(\frac{R}{r})^2 - 3(\frac{R}{r})^4]sin2\theta$$

Considering the pressure applied at the plate boundaries, defined as $P = q/t = 2.5e8\,N/m^2$, and appropriately evaluating the circular coordinates (r, θ) it is possible to analytically compute the stress field at any point within the domain.

In particular, by assuming $\theta = -\frac{\pi}{2}$ and expressing $\sigma_{\theta\theta}$ as a function of r the stress distribution along the horizontal axis of the x-y coordinate system between points A and B can be calculated as:

$$\sigma_{\theta\theta}(r) = \frac{P}{2}[1 + (\frac{R}{r})^2] + \frac{P}{2}[1 + 3(\frac{R}{r})^4]$$

The resulting distribution follows the trend shown in the figure 2, from which the stress values at points A and B, the endpoints of the sub-domain under consideration, can be identified as:

$$\sigma_{\theta\theta}(A) = \frac{P}{2}[1 + (\frac{R}{r})^2] + \frac{P}{2}[1 + 3(\frac{R}{r})^4] = 3P = 7.5e8\,N/m^2$$

$$\sigma_{\theta\theta}(B) = \frac{P}{2}[1 + (\frac{R}{r})^2] + \frac{P}{2}[1 + 3(\frac{R}{r})^4] = P = 2.5e8\,N/m^2$$

Furthermore, the same quantity can be evaluated at point C ($r = R, \theta = 0$), $\sigma_{\theta\theta}(C) = -P = -2.5e8\,N/m^2$ and at point D. In the latter case, the computation is unnecessary, since in proximity to the loaded boundary the stress assumes a value equal to the applied external load.

The objective of this report is to determine the same solutions obtained analytically by means of the Finite Element Analysis Program (FEAP). The computational analysis, which—by exploiting the symmetry of the problem—will be restricted to one quarter of the entire domain (bounded by points A, B, C, and D), will be carried out through different discretization methods:

- Triangular plane stress elements;
- Rectangular plane stress elements;

For each element type, analyses will start from a coarse discretization and will progressively be refined in both the vertical and horizontal directions. Finally, the convergence of the computed tip stresses to the analytical solution will be assessed.

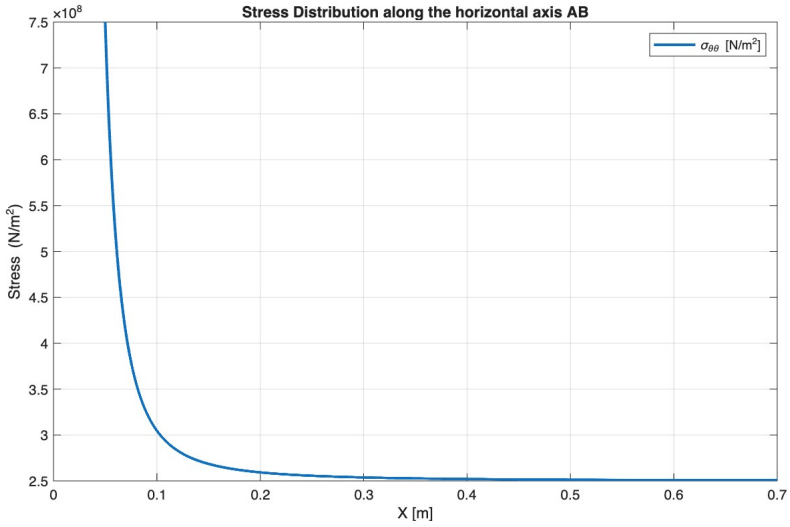

Figure 2: Stress distribution along the horizontal axis AB.

3 Finite Element Analysis with 3-Nodes Triangular Elements

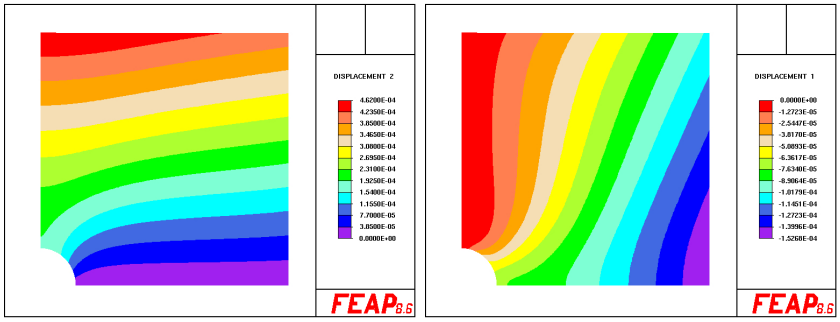

(a) Vertical displacement (b) Horizontal displacement

Figure 3: Computed vertical and horizontal displacement distributions

To minimize the computational effort, the geometric symmetry of the problem was exploited so that only one quarter of the domain was analyzed. This assumption requires the application of symmetry boundary conditions: nodes along side AB and side CD are constrained with sliding supports, enforcing zero vertical displacement on AB and zero horizontal displacement on CD. Figure 3 depicts the correct implementation of these boundary conditions.

The resulting stress distribution is presented in Figure 4. The color maps of the vertical and horizontal stress components were generated with a mesh refinement of 64, ensuring an accurate representation of the stress field.

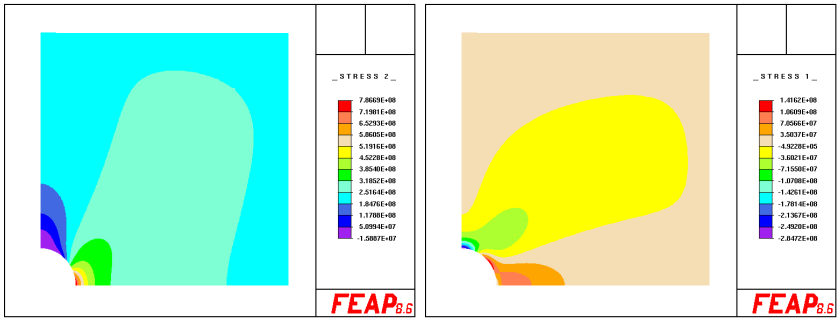

(a) Vertical stress (b) Horizontal stress

Figure 4: Computed vertical and horizontal stresses distributions

From the computational analysis, it was possible to evaluate the stress values at points A, B, and C, and to compare the results with the corresponding analytical solutions. With a mesh refinement level of 64, the following stress values were obtained:

- $\sigma_y(A) = 7.8136e8\, N/m^2$
- $\sigma_y(B) = 2.3143e8\, N/m^2$
- $\sigma_x(C) = -2.8472e8\, N/m^2$

Furthermore, Figure 5 presents the data describing the evolution of the percentage error with respect to the analytical solutions for each point, as a function of the different mesh refinement levels considered.

In contrast to the expected behavior and to the findings reported in "Homework 01 – Cantilever Beam", increasing the mesh refinement did not result in a consistent decrease of the error. For point B, the minimum deviation from the analytical solution occurred at mesh refinement = 1, whereas for the other two points the lowest error was observed at mesh refinement = 10. Beyond this level, further mesh refinement led to increasing discrepancies with respect to the analytical results.

We can therefore conclude that the FEM analysis based on linear three-nodes triangular elements does not converge to the exact solution, even when employing a mesh refinement of 64.

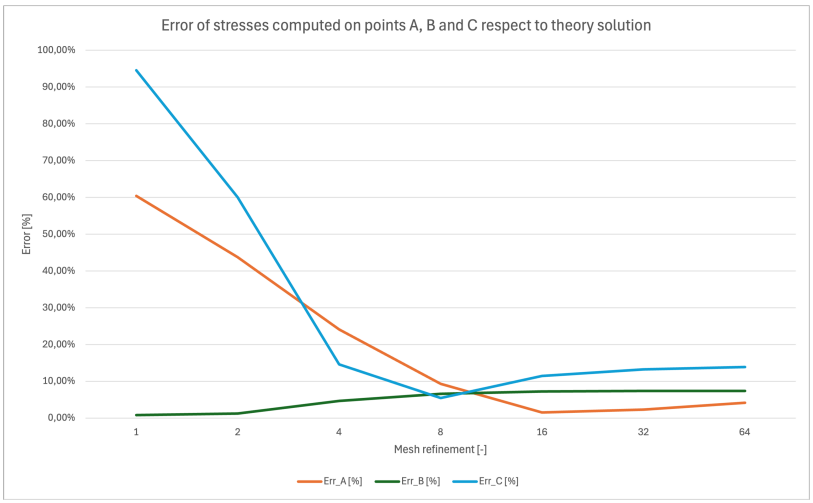

Figure 5: Error distribution in points A, B and C respect to analytical solution (linear triangular elements)

4 Finite Element Analysis with 4-Nodes Rectangular Elements

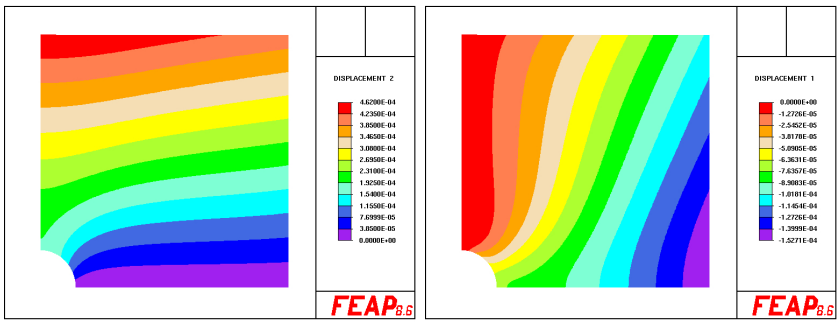

(a) Vertical displacement (b) Horizontal displacement

Figure 6: Computed vertical and horizontal displacement distributions

The problem of the plate with a circular hole was also analysed using linear four-node rectangular elements. As in the previous case, the boundary conditions were verified prior to performing the analysis: along side AB the vertical displacement is constrained to zero, while along side CD the horizontal displacement is constrained to zero, as illustrated in Figure 6. Consequently, the boundary conditions associated with the chosen subdomain have been correctly implemented.

In addition, both the displacement color maps and the vertical and horizontal stress distributions shown in Figure 7 clearly indicate that the use of linear four-node rectangular plane-stress elements significantly improves the accuracy of the computed results.

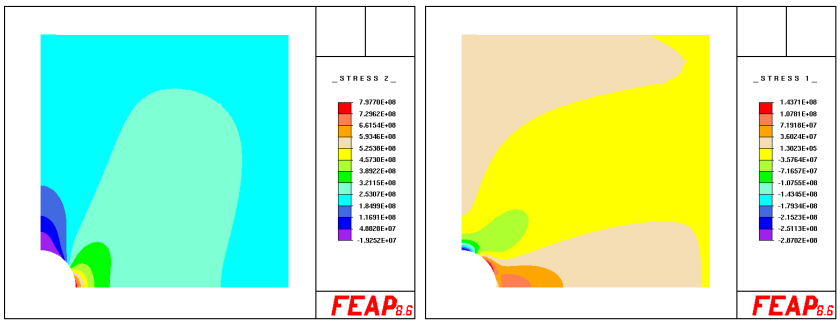

(a) Vertical stress σ_y (b) Horizontal stress σ_x

Figure 7: Computed vertical and horizontal stresses distributions (linear rectangular elements)

Compared to triangular elements method, the rectangular formulation exhibits superior convergence behavior, as it allows for a more accurate representation of stress gradients, particularly in regions where these gradients vary rapidly, such as near the hole boundary. The resulting stress distribution displays a more refined and physically realistic gradient around the hole, capturing the stress concentration zones more effectively than the triangular formulation. Nevertheless, although the resolution is significantly improved, the peak stress at the hole edge still shows a slight deviation from the theoretical prediction.

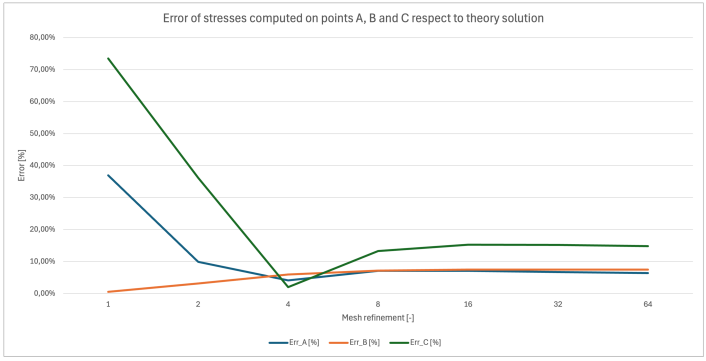

Figure 8: Error distribution in points A, B and C respect to analytical solution (linear rectangular elements)

The analysis of the percentage error at points A, B, and C as a function of mesh refinement (Figure 8) confirms the superior effectiveness of this second

FEM discretization strategy compared with the triangular-element approach. The acceptability threshold, set at 5%, is achieved with a significantly lower number of rectangular elements (approximately mr = 5). However, even in this case, further mesh refinement does not lead to improved convergence of the computational results toward the corresponding analytical values.

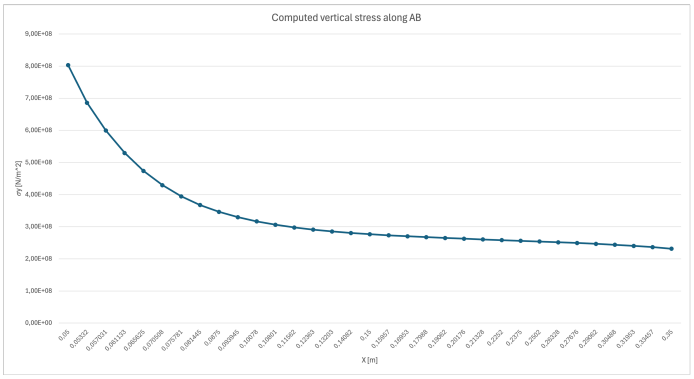

(a) Vertical stress σ_y distribution on AB

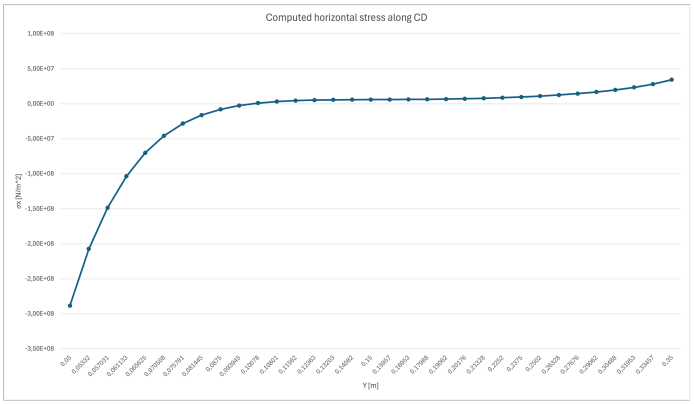

(b) Horizontal stress σ_x distribution on CD

Figure 9: Computed vertical and horizontal stresses distributions

Figure 9 presents the distributions[1] of the vertical and horizontal stress along sides AB and CD, respectively. The results show that, although the stress values at the endpoints (corresponding to nodes A, B, C, and D) do not coincide with those obtained analytically, the overall trend of the computed curves closely reproduces the analytical solution shown in Figure 2.

[1]Both the distributions were computed with mr = 32.

5 Conclusion

The analysis of a plate with a circular hole subjected to uniaxial tension has been carried out through both analytical solutions (Kirsch's equations) and finite element simulations using different discretization strategies. The comparison between the analytical stress field and the numerical results demonstrates that, while the FEM solutions reproduce the qualitative behavior of the stress distribution, including the characteristic concentration near the hole, the quantitative agreement varies significantly depending on the type of finite elements employed.

Triangular three-node linear elements exhibited limited convergence properties and failed to approximate the analytical values accurately, even under substantial mesh refinement. In contrast, linear four-node rectangular plane-stress elements displayed superior performance, achieving acceptable accuracy with fewer elements and capturing more effectively the stress gradients in regions of rapid variation. Nonetheless, neither formulation was able to reproduce exactly the peak stress values at the boundary of the hole.

This deviation at the boundary points can be attributed to limitations of low-order finite elements. Since stresses are computed through differentiation of the displacement field, numerical inaccuracies become amplified, especially in the presence of steep gradients or near-singular behavior. Furthermore, the finite element discretization cannot fully replicate the analytical stress singularity at the hole boundary, leading to local discrepancies despite a globally accurate trend.

Overall, this analysis underscores the importance of element choice when modelling problems involving stress concentration. While low order rectangular elements provide a substantial improvement over triangular ones, achieving precise boundary stress values may require higher order formulations.